Energy 244 (2022) 123185

Contents lists available at ScienceDirect

Energy

journal homepage: www.elsevier.com/locate/energy

Modelling of cooling radiant cubicle for an office room to test cooling performance, thermal comfort and energy savings in hot climates

Nagham Ismail, Djamel Ouahrani*

Department of Architecture and Urban Planning, College of Engineering, Qatar University, P.O. Box 2713, Doha, Qatar

ARTICLE INFO

Article history:
Received 24 June 2021
Received in revised form
3 December 2021
Accepted 10 January 2022
Available online 12 January 2022

Keywords:
Radiant cooling
Personal thermal comfort
CFD
Mathematical model
Cooling energy
Energy savings

ABSTRACT

The building industry challenges have led researchers to develop a personalized conditioning system aiming to create a microclimate comfort zone around the occupant. Radiant cooling become prevalent due to their potential in affording both comfort and energy saving. Consequently, this study investigates the performance of a personalized cooling radiant cubicle (PCRC) combined with a conventional heating, ventilation, and air-conditioning (HVAC) system in an office room in hot climates. PCRC performance is assessed by introducing a novel model that combines computational fluid dynamics (CFD) and mathematical simulation based on two criteria: the ability in creating a thermal comfort zone near the occupant at high set-point temperatures and the economic feasibility in terms of energy savings and payback period. The results demonstrate that PCRC (i) maintains a comfortable personal thermal environment in the desired zone (ii) reduces the thermal asymmetry (iii) improves the corresponding predicted percentage of dissatisfied (PPD) index. When compared to published experiment, it is shown that the developed model is valid with a maximum relative error of 5% underlining its accuracy and eliminating the need of a full-physics based model. Moreover, implementing PCRC reduces cooling energy by 18% compared to conventional system with a payback period between 6 and 7 years.

1. Introduction

Energy savings and occupant thermal comfort are considered the main issues in building technology; thus, the development of energy efficient heating, ventilation, and air-conditioning (HVAC) systems and their control strategies are continuously evolving in HVAC industry [1,2]. Nevertheless, the common way adopted to define operational settings for HVAC systems is to use fixed setpoint temperature, which assume occupants' static comfort conditions [3]. These fixed setpoint ranges are often narrow, around 2 K, 2 °C (4 F); even though they do not result in higher occupant satisfaction than environments with wider ranges, such as 4–6 K (7–10 F) [4]. Researchers justified these findings by the fact that both the predicted mean vote (PMV) and the adaptive models, used to indicate the thermal comfort zone, provide an averaged response of a population without accommodating the occupant's individual preferences [5–7]. Moreover, new knowledge has been gathered regarding metabolic health effects of temperature exposure outside the well-known comfort zone. It is shown that the trend towards higher temperatures in summer and lower temperatures in winter can have significant effects in promoting metabolic health and fighting the diseases related to metabolic syndrome [8]. Therefore, recent studies' objective was to implement wider temperature ranges without compromising the occupants' thermal comfort [4–9]. The primary benefit of widening the thermostat setpoint range is to lessen energy consumption by the building's HVAC system. For instance, Hoyt et al. found that reducing the heating setpoint by only 1.1 $^{\circ}C$ saves an average of 34% of terminal heating energy while keeping occupant thermal satisfaction [4]. Furthermore, according to Brager et al. simulation results, if new strategies and systems were to allow the building operator to expand the range of temperatures at which occupants are comfortable, the annual central HVAC energy consumption can be reduced by roughly 10% per 1$^{\circ}C$ of expansion in either direction [10]. From here comes the importance of shifting towards new energy-efficient paradigms that allow the expansion of setpoint temperatures range in buildings while providing enhanced occupant' thermal experiences.

In recent years, researches emerged in developing new strategies that maintain the thermal comfort while saving air

* Corresponding author.
E-mail address: djamel@qu.edu.qa (D. Ouahrani).

https://doi.org/10.1016/j.energy.2022.123185

Nomenclature

A_{rad}	area of the radiant surface (m^2)
c_p	specific heat (J/kg. K)
CFD	computational fluid dynamics
C_t	equation constant
Di	inner pipe diameter
Do	outer pipe diameter
h_{conv}	heat convection coefficient (W/m^2. K)
h_{rad}	heat radiation coefficient (W/m^2. K)
k	thermal conductivity (W/m. K)
L	length
Lc	characteristic length
$\dot{m}$	mass flow rate (kg/s)
Nu	Nusselt number
n	number of pipes
n_y	number of nodes in y-direction
NPV	net present value ($)
PCRC	personalized cooling radiant cubicle
PCS	personal comfort system
PMV	predicted mean vote
PPD	predicted percentage of dissatisfied people
Q	heat transfer rate (W)
Ra	Rayleigh number
Re	Reynolds number
Pr	Prandl number
T	temperature (°C)
V	velocity (m/s)
W	width (m)
x	horizontal position (m)
y	vertical position (m)

Greek Symbols

Δx	node thickness in x-direction
Δy	node thickness in y-direction
σ	Stefan-Boltzmann coefficient
ε	emissivity
ρ	density (kg/m^3)
μ	dynamic viscosity (Pa.s)

Subscripts

air	air
conv	convection
convf	forced convection
convn	natural convection
crc	cooling radiant cubicle
in	inlet water temperature
inner	inner node
outer	outer node
p	pipe number
principal	principal node
r	room
rad	radiation
water	water
x	x-coordinate
y	y-coordinate

conditioning energy. These promising paradigms are based on localized thermal conditioning of occupants' bodies, and they are called personal comfort systems (PCS) [11]. These attempts offered opportunities to move the indoor thermal environment control from the “one-fits-all” approach to the occupant-centric merits [12]. On the one hand, PCS provides occupants with the opportunity to meet their own personal preferences, on the other hand the ‘corrective power’ of localized conditioning affords comfort over a wider range of ambient temperatures leading to large energy savings [10,13]. PCS arises in different forms and systems targeting sensitive body parts that can have a considerable effect on the whole-body thermal comfort and leading to higher acceptance of wider temperature excursions [7,13]. Typical PCS cooling takes place through convective personalized ventilation [14] or through cooled chairs [15,16]. Besides, typical PCS heating is provided by heated chairs [17], radiant personal heater and foot warmers [18].

An energy-efficient personal comfort system (PCS) is typically based on radiant cooling/heating used to insure thermal comfort with lower energy consumption [19,20]. This is because radiant air conditioning systems can generate an indoor environment, which has smaller vertical temperature differences and almost no air movement field avoiding local thermal discomfort [21]. However, radiant heating and cooling systems are considered complicated since they involve different heat transfer mechanisms. This introduces certain complexity when a radiant heating/cooling model is integrated into a building energy simulation [22]. Despite this fact, Computational fluid dynamics (CFD) was shown to be a powerful tool in investigating the thermal performance of radiant panels. Zhou et al. performed experiments and CFD simulations to assess the thermal performance of a low-temperature radiant floor heating system assisted with variable heat storage materials and heating pipes implemented to a room's floor structure [23]. They found that CFD simulations were able to model the different physics involved giving validated results in agreement with performed experiments. Peng et al. proposed to use a radiant ceiling-sidewall composite assisted by a heat pump [24]. Variable installation configurations of the system were studied by (CFD) simulations which were able to predict the temperature distribution within the space. Karacavus et al. performed a CFD study in an office on local and general thermal comfort for variable positions of radiant panels: below the window and on the ceiling [24]. In their work, the effects of panel temperature and heat flux were investigated using CFD simulations. It was shown that local and general comfort levels were largely affected by outdoor temperature. Xie et al. studied the thermal performance of capillary ceiling cooling panel [25]. They considered the effect of thermal load distribution, and water mass flow rate on ceiling surface temperature and indoor environment thermal comfort [26]. Mustakallio et al. investigated numerically and experimentally an innovative system consisting of a radiant panel integrated with a chilled beam [27]. They concluded that radiant panel heating can be used in cold climates. Catalina et al. evaluated thermal comfort in a room characterized by a cooling ceiling through PMV model using inputs from CFD simulations and experimentation [28]. The system insured acceptable thermal comfort within different regions of the room. However, in the majority of these studies, the radiant panels were placed at ceiling or at floor level. Modest attempts in literature have considered the investigation of cooling radiant panels in other locations surrounding the human body. For instance, Du et al. proposed to implement a cooling radiant panel at the proximity of the occupant in a sleeping room constituting a task/ambient air condition system [29]. Consequently, the system was able to create local comfortable environment profiting from the sleeping person's immobility which induced considerable energy savings [29]. Du et al. investigated the effects of changing the radiant panel's operational and design parameters on thermal comfort and energy consumption [30]. Their parametric study involved the temperature at the surface of the radiant panel, its emissivity, its area and the distance separating the radiant panel from the bed. Vaibhav Rai khare and his team were the pioneer in studying the radiant-based personalized cooling system using the principle of radiant cooling integrated with the conventional all-air system to achieve better thermal environment at the workspace [31, 32]. In this way, they introduced a cubicle consisting of radiant panels where chilled water is circulating through copper tubes and the heat transfer from the working fluid is setup by radiation and conduction. By using such system in the near vicinity to control the microclimate around the occupant, the set point temperature of the background HVAC system can be increased leading to energy savings. Thereafter, they combined the radiant cooling system with other radiant systems like the radiant ceiling conditioning system and found that this combination could also fulfill the requirement of thermal comfort in an efficient way [19, 33].

In this study, a novel model that employs a combination of a computational fluid dynamics model (CFD) and mathematical simulation is developed to assess the performance of a personalized cooling radiant cubicle (PCRC) introduced at the proximity of an occupant in an office space located in hot climates taking advantage of the occupant immobility during working hours. The key novelty of the model approach that distinguish it from existing methods can be summarized as follows:

- This model captures the variation of the chilled water temperature in the PCRC by solving the energy conservation equations of PCRC using a novel mathematical model coupled to CFD.
- Adopting a simplified but robust model increases the expectation in providing: (i) accurate predictions compared to the constant chilled water temperature CFD model (ii) low computational cost and time compared to a full-physics based CFD model.
- The assessment of performance is based on two main criteria: (i) the ability of PCRC system in creating a thermal comfort zone near the occupant at relatively high set-point temperatures (ii) the economic feasibility of the proposed PCRC system in terms of energy savings and pay-back period.

Hence, the originality of this study is in providing a reliable and low-cost computational tool for assessing the performance of a personalized cooling radiant cubicle (PCRC) in (i) providing the occupant comfort (ii) and allowing a significant increase of the energy savings by increasing the supply air temperature of HVAC system. The CFD model developed is simulated using the commercial software ANSYS Fluent and the resultant thermal and fluid parameters are coupled to the mathematical model solved on MATLAB software and to PMV and PPD models to investigate comfort conditions. Then, the integrated model is used to conduct a case study highlighting the efficiency of introducing the PCRC to a conventional HVAC system compared to a base case without PCRC. The integrated model is validated by comparing the thermal profile at the vicinity of the human body with published experimental data. Finally, an economic analysis is conducted to assess the energy savings associated with the proposed system and the pay-back period is computed.

2. System description

In this study, the performance of personalized cooling radiant cubicle (PCRC) with conventional air conditioning system is evaluated in order to identify the associated cooling energy saving while maintaining the personal thermal comfort of the occupant. PCRC is placed at the vicinity of the occupant and consists of three panels surrounding the occupant desk where chilled water at relatively low temperature is circulating through tubes absorbing heat by convection and radiation. Fig. 1(a) illustrates the configuration of the described system applied on a typical office space with one occupant, desk, chair, and computer while Fig. 1 (b) presents the schematic of the proposed system consisting of a water pump circulating the water in the PCRC and a portable radiant chiller to cool down the water. It is noteworthy that each radiant cubicle is well insulated on all sides that are unexposed to the occupant body in order to minimize the useless heat transfer [34]. Whereas the exposed sides are covered by aluminum sheet painted by an acrylic matt spray with high emissivity [35]. The aluminum sheet is glued on the water pipes and between them.

3. Research methodology

This study aims to develop a valid model simulating the performance of the cooling radiant cubicle in a typical office in hot climates such as Doha, Qatar. In order to achieve this goal, the research methodology begins by developing a computational fluid dynamics (CFD) model that simulates the thermal and fluid profiles resulting from the presence of radiant cubicle in a typical office space in Doha, Qatar (Section 3.1). This CFD model is coupled to a mathematical model that solves the energy equations of the cooling radiant cubicle and provides the needed boundary conditions to the CFD model and to a thermal comfort model. The governing equations of the mathematical model will be elaborated in Section 3.2 based on the assumptions adopted. Therefore, in the following, the CFD model of the typical office space with radiant panels, and the mathematical model simulating the PCRC energy performance

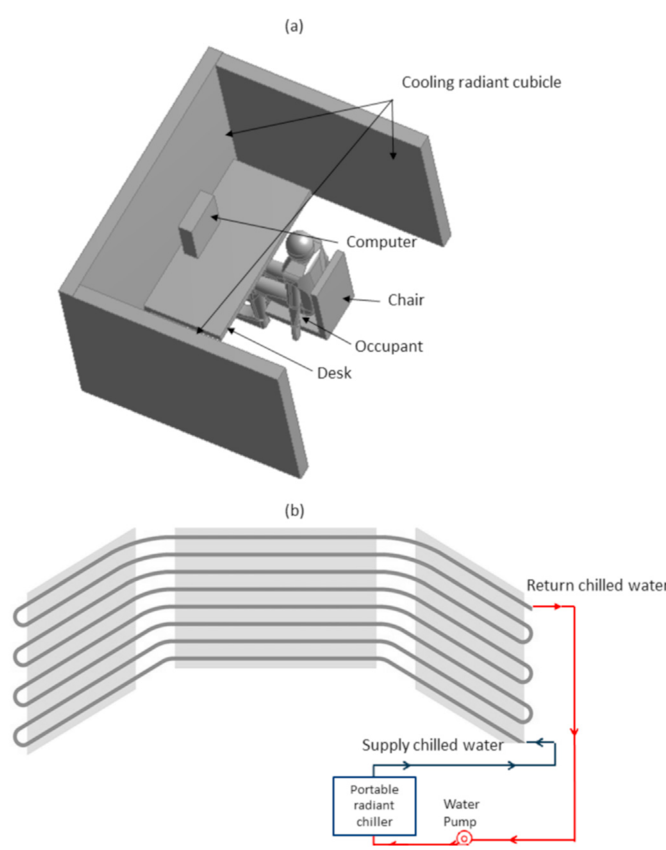

Fig. 1. Schematic of (a) the cubicle set-up surrounding the occupant and (b) the proposed system components.

are presented separately; afterwards, a section on the integration methodology that combines both models until convergence to find the associated thermal comfort is demonstrated. To ensure the validity of the integrated model, the simulation results are compared to a published experiment [31]. Finally, an economic feasibility study of the proposed PCRC system is established to evaluate its pay-back period and energy savings over the conventional cooling system case.

3.1. CFD methodology

Implementing cooling radiant cubicle in an office space equipped with a conventional mixing configuration involves complex physics of airflow and temperature fields [22]. Since CFD modelling has proved high efficiency in the computation of velocity and temperature fields, it was selected in this study to test the performance of PCRC in reducing energy consumption in an office space equipped with conventional air conditioning system without compromising the thermal comfort of the occupant.

CFD modelling is mainly constituted of three phases: (i) preprocessing where the geometry and meshing are created, (ii) processing where appropriate models are selected and accurate boundary conditions are provided to numerically solve the fluid flow equations in the computational domain and (iii) postprocessing where results are generated.

Therefore, in order to compute the air flow and temperature fields resulting from implementing cooling radiant cubicle in an office space, a 3D detailed CFD model was developed using the commercial ANSYS Fluent 19 software.

3.1.1. Geometry and meshing

A small typical office space was drawn in design modeller of ANSYS Fluent software. Inlet and outlet air conditioning diffusers were placed at ceiling level. Only one external wall directed to the south has a glazed window. An occupant modeled by a thermal manikin sits on its desk and is surrounded by PCRC to create a comfortable microclimate around him. All the geometrical dimensions of the office space are shown in Table 1. Fig. 2 (a) shows the geometry drawn before generating the mesh. Afterwards, the created geometry was meshed using tetrahedral elements resulting in 2539157 number elements and 477932 number nodes. Mesh quality and size are indispensable in obtaining accurate results and minimizing simulation errors. The mesh quality is achieved by maintaining appropriate element quality, low levels of element skewness, and proper orthogonal quality [36]. Moreover, several refinement techniques were used to enhance the quality of the mesh.

A grid independence test was performed to select the appropriate mesh refinement. Face sizing of 2 cm at walls, desk, inlet and outlet while face sizing of 1 cm was used for radiant panels and thermal manikin since these surfaces are critical and largely affect the microclimate environment. Furthermore, surface inflation was used near surfaces characterized by a growth rate of 1.1 and number of layers equal to 6. The surface inflation contributes to the capture of boundary layer development near surfaces and enhances the prediction of airflow and thermal patterns. Consequently, the average of the Element Quality is obtained as 0.96 and the minimum was 0.56; the average Skewness is 0.224 and the maximum was 0.882; the average Orthogonal Quality is 0.96 whereas the minimum was equal to 0.59. Fig. 2 (b) illustrates a meshed section plane of the office space.

Table 1
Geometrical dimensions of the office space.

Office floor dimensions	3.4 m × 3.4 m
Office height	2.6 m
Cooling radiant cubicle surface area	6 m^2 (1.2 × 1.5 + 1.2 × 2 + 1.2 × 1.5)
Window's surface area	1 m^2
Grill surface area	1.9 m^2

3.1.2. Airflow modelling

Flow physics are affected by different factors such as boundary layers' development, buoyancy, and turbulence which should be appropriately modeled. Furthermore, controlling the resolution of the grid at the proximity of surfaces is important to trap the formation of fluid and thermal boundary layers. ANSYS Fluent software solves the Navier-Stokes equations governing the airflow/thermal fields by using numerical analysis based on finite volume method, and provides variable turbulence models and discretization techniques. The realizable k-ε turbulence model is one of the most commonly used turbulence models and has proved its efficiency in modelling indoor ventilated environments. For this reason, it was chosen in this work to model turbulence effects. To solve the momentum, energy, turbulent kinetic energy k, and rate of dissipation of turbulent kinetic energy ε equations, second-order upwind discretization scheme is selected. Since the indoor fluid is steady, incompressible, and characterized by relatively low speed, pressure-based solver is used. Computation of pressure in the domain is performed using the "PRESTO" staggered scheme [37,38]. Air density variation is modeled using the incompressible ideal gas law. For coupling of velocity and pressure in the computational domain, the SIMPLE algorithm is adopted [37].

Flow and thermal boundary layers are constituted by several sub-layers: the laminar sub-layer, the buffer sub-layer and the turbulent sub-layer. In order to capture these different sub-layers, the enhanced wall treatment option is used enabling to switch, as function of the grid size, between the two-layer model resolving for the viscous sub-layer and the enhanced wall functions used in the transition sub-layer [39–41].

3.1.3. Radiation modelling

ANSYS Fluent offers six models to implement the radiative heat exchange. Among these models, the surface to surface (S2S) and the discrete ordinates (DO) models are the most used for the thermal field computation in indoor spaces involving radiant air-conditioning systems [42–44]. In S2S model, heat transfer by radiation occurs in a closed environment between grey emissive surfaces [45]. In DO model, the radiative transfer equation is resolved for a finite number of discrete solid angles, each associated with a fixed vector direction in the global Cartesian system [46]. The DO model represents several advantages over the S2S model. First, convergence of the radiative heat transfer finite volume scheme is accelerated [44]. Second, S2S only considers the radiation process between surfaces without taking into account the presence of air in the space [47]. It was shown that the DO model is highly accurate in the computation of the radiant intensity field for optically thin media where air is treated as a participating media characterized by an extinction coefficient equal to zero [48]. Therefore, in this study the DO model was used for radiation modelling.

3.1.4. Boundary conditions

Boundary conditions for energy and airflow are inputs that should be provided to the CFD model. The computation of temperature distribution inside the office space requires specification of heat fluxes from surfaces (walls and window) along with the heat flux generated from electrical equipment, thermal manikin simulating a seated human body and any other heat source. Only one wall is considered external (with glazed window) and the three

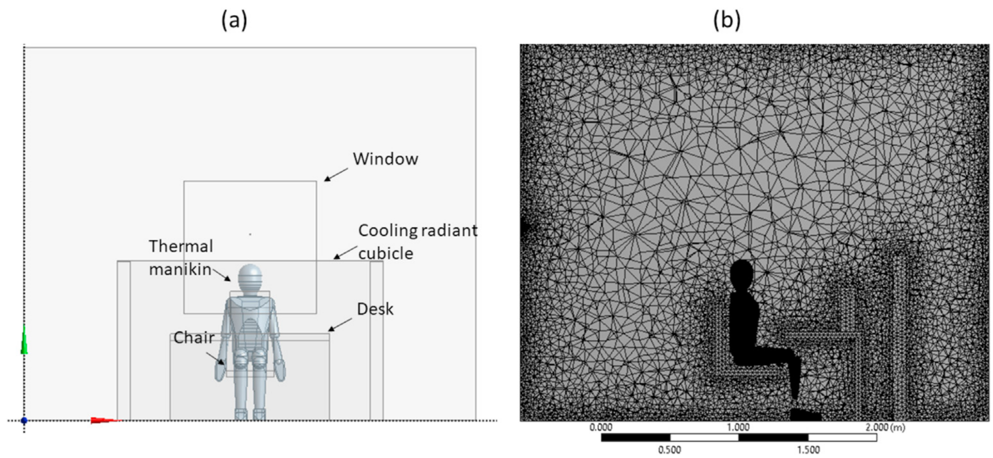

Fig. 2. Geometry of the typical office space equipped with PCRC generated on ANSYS Fluent (a) before meshing (b) after meshing.

other walls are considered internal (partition walls). Since the office space is equipped with conventional air-conditioned system, both inlet and outlet were placed at the ceiling level. The supply diffuser is considered as velocity inlet with specified inlet temperature. On the other hand, the outlet diffuser is modeled as pressure outlet with zero gage pressure. Finally, a constant temperature is specified as boundary condition for PCRC inner side while zero heat flux is considered for all other insulated sides. All the heat fluxes imposed at the external wall, the window, the internal walls, the ceiling, the floor, the thermal manikin heat generated, and the electrical equipment heat flux are specified in Table 2.

3.1.5. Convergence and error analysis

Each simulation is run until reaching steady state conditions. The numerical convergence is determined according to several criteria. First, the scaled residuals for continuity and momentum are reduced to less than 10^{-5}, except for energy where the scaled residuals are less than 10^{-6}. Second, the velocity and temperature at five random locations in the space should be monitored to verify the solution stability and convergence. Moreover, a grid independency test consisting of five grid sizes corresponding to five number of elements (119 483, 238966, 358449, 477932, 597415) has been conducted to make sure that the results are independent of grid resolution. The results show that the percentage difference of velocity and temperature at five random locations between the grids with 477932 and 597415 elements does not exceed 0.6%. Hence, the grid size that corresponds to 477932 number of elements was considered fine enough and used for running all the current simulations. Finally, the satisfaction of conservation laws is tested by examining the overall mass, momentum, and energy balances. The maximum net imbalance is related to the mass conservation and it is obtained to be around 0.0908% (<0.2%) of the net flux through the whole domain when the solution has converged; satisfying consequently the conservation laws.

3.2. Mathematical model of PCRC

As mentioned previously in section 3.1.4, the CFD model requires specified boundary conditions in order to solve the momentum and energy equations in the computational space. Among these boundary conditions, the temperature of PCRC must be provided. However, as chilled water circulates inside the cubicle, the temperature of water increases by absorbing the heat from the adjacent air by convection, as well as the heat released by radiation from the surrounding surfaces. Therefore, it is of interest to find the average temperature of PCRC. From here comes the importance of a simplified mathematical model that solves the energy balances across PCRC to find its average temperature in order to be used as boundary condition in the CFD model.

3.2.1. Physical configuration

As shown in Fig. 1 (b), the PCRC consists of tube elements where chilled water is flowing. In radiant heating/cooling systems, the tubes can be laid out in different patterns [22]. The two most used patterns are serpentine and spiral. In this study, the serpentine pattern is used; thus, the heat transfer is mostly in the transversal direction that is perpendicular to the tubing plane. For sake of simplicity, the PCRC shown in Fig. 1 (b) is open as if it lies in the same plane. Fig. 3 (a) illustrates the physical configuration of the PCRC where the average tube length in the circuit is denoted by *L*,

Table 2
Boundary conditions used in CFD simulation.

Boundary condition	Type of boundary condition	Value
External wall	Heat flux	15 Wm^2 [49]
Internal walls and floor	Heat flux	0 W/m^2
Glazed window	Heat flux	30 W/m^2 [50]
Inlet Grill	Velocity inlet	0.75 m/s [51]
	Temperature inlet	18 °C
Outlet Grill	Pressure outlet	–
Lighting (ceiling)	Heat flux	10 W/m^2 [52]
Computer	Heat flux	90 W [53]
Thermal manikin	Heat flux	1 MET [54]
PCRC (at the occupant side)	Constant temperature	14 °C (Initial guess)
PCRC (at all other insulated sides)	Heat flux	0 W/m^2

the outer and inner diameter are respectively D_o and D_i, and the tubes are uniformly spaced by a distance W. The chilled water enters the radiant panel through the inlet tube at relatively low temperature T_{in}. When water flows across the tubes, the temperature of the water increases as it exchanges heat with the adjacent medium.

Four main assumptions are adopted according to Laouadi et al. [22] that help developing the simplified mathematical model:

(i) No gradient in temperature is considered along z-axis (the length of the tube). This assumption is valid when the tube spacing is neglected compared to the tube length ($W/L \lll\lll 1$).
(ii) Since the tube thickness is small compared to the internal diameter ($(Do\text{-}Di)/Di <<<< 1$); thus, no gradient in temperature is considered within the tube material.
(iii) The unexposed side as well as the edges of the radiant panel are all adiabatic (well insulated).
(i) The heat balance equations are considered under steady state condition since all the input parameters are constant with respect to time.

Based on the above assumptions, two-dimensional model is developed (in x-y plane). As shown in Fig. 3 (b), for each y, a three-node model is established in x-direction. As per its name, this three-node model consists of three nodes in x-direction: one for the insulated adiabatic surface that is unexposed to the human body environment and it is called the outer node, one for the highly conductive exposed surface and it is called the inner node, and one for the intermediate medium between the outer and inner nodes and it is called the principal node. The last node is called principal because it includes the water pipe where chilled water flows and absorbs the heat from the adjacent medium. The number of water pipes n is given by the following equation:

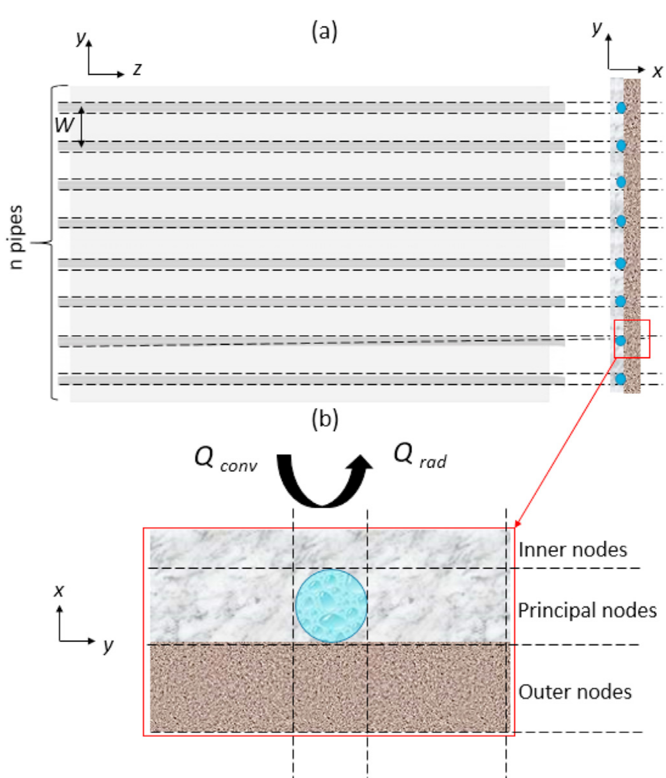

Fig. 3. Physical configuration of the adopted model showing (a) front and top views of the cooling radiant cubicle (b) the three-node model adopted.

$$n = A_{rad} \,/\, (L * W) \tag{1}$$

where A_{rad} is the surface area of the radiant panel. In addition to the water pipe, the principal node includes also the space between the water pipes where the aluminum sheet is glued to the insulation. As shown in Fig. 3 (b), the outer node is adiabatic (well insulated); thus, no heat transfer occurs across this node. Contrarily, the principal node, where the chilled water flows, exchanges heat with the inner node exposed to the environment. At its turn, the inner node exchanges heat with the environment by convection and radiation.

3.2.2. Mathematical formulation

In order to achieve the objective of this section which is to compute the average surface temperature of the PCRC, the energy equations of each node in the three-node model at each y should be developed and solved.

3.2.2.1. Inner node. As described previously and shown in Fig. 3 (b), the inner node absorbs heat by convection and radiation from the exposed environment and releases the heat to the principal node by conduction. Therefore, the energy equation at the inner node is as following:

$$-k_{inner} L \Delta x_{inner}\, dy \frac{\partial^2 T_{inner}(y)}{\partial y^2} - k_{inner} L\, dy \frac{\left(T_{principal}(y) - T_{inner}(y)\right)}{\Delta x_{inner}} = h_{conv} L\, dy\, (T_r - T_{inner}(y)) + h_{rad} L\, dy\, (T_r - T_{inner}(y)) \tag{2}$$

where the first and second term stand for the conduction heat transfer that occurs respectively between the inner nodes in y-direction and between the principal node and the inner node. The third term (first term after equal sign) represents the convection heat transfer with the room air and the last term represents the radiation heat transfer. It is noteworthy that the convection coefficient h_{conv} must stand for both forced and natural convection with the room air (mixed convection). The forced convection coefficient is related to the velocity of air flowing over the radiant panel. Therefore, the forced convection coefficient h_{convf} is deduced from the correlation of Nusselt number Nu [55]:

$$Nu_f = \frac{h_{conv_f} L_c}{K_{air}} = 0.664\, Re^{0.5}\, Pr^{\frac{1}{3}} \text{ if } Re < 10^5 \tag{3 a}$$

$$Nu_f = \frac{h_{conv_f} L_c}{K_{air}} = 0.037 Re^{0.8}\, Pr^{\frac{1}{3}} \text{ if } Re \geq 10^5 \tag{3 b}$$

where the characteristic length L_c is the hydraulic radius of the panel surface computed as the ratio of the surface area to the perimeter of PCRC [56]; K_{air} is the air thermal conductivity, Re and Pr are respectively the Reynolds and the Prandl numbers of air given as follows:

$$Re = \rho_{air} V_r L_c / \mu_{air} \tag{3 c}$$

$$Pr = 0.7 \tag{3 d}$$

where ρ_{air} and μ_{air} are the air density and dynamic viscosity at room temperature while V_r is the velocity of air near the PCRC system.

According to Drojetzki et al. the natural convection coefficient h_{convn} in cooling mode is found using the following correlation [57]:

$$Nu_n = \frac{h_{conv_n} L_c}{K_{air}} = 0.835\ C_t Ra^{0.25} \tag{4 a}$$

where C_t is the equation constant that is equal to 0.515 (for air), Ra is the air Raileigh number given as follows:

$$Ra = \frac{\rho_{air} g \beta_{air} (T_{crc} - T_r)}{\mu_{air} \alpha_{air}} L_c^3 \tag{4 b}$$

where β_{air} and α_{air} are respectively the coefficient of thermal expansion and thermal diffusivity while T_r is the temperature of air near the PCRC system. T_{crc} is the average temperature of the cooling radiant cubicle computed as follows:

$$T_{crc} = \frac{1}{nW} \int_0^{nW} T_{inner}(y) dy \tag{5}$$

Therefore, h_{conv} resulted from the mixed convection heat transfer between PCRC and the room air is given by the sum of both the forced convection h_{convf} and the natural convection h_{convn} coefficients.

The radiation coefficient h_{rad} was found by linearizing the well-known Stefan-Boltzman equation resulting in an exchange radiation coefficient as following [58]:

$$h_{rad} = 4 \varepsilon \sigma T_{inner}^3(y) \tag{6}$$

where ε, and σ are respectively the emissivity and the Stefan-Boltzmann coefficient.

3.2.2.2. Principal node. Chilled water is flowing inside the tubes embedded in the insulation and covered by an aluminum sheet painted with high emissivity acrylic matt. When water flows across the tubes, its temperature increases as it absorbs heat from the adjacent medium. The number of water tubes is computed in Eq. (1). The water tubes are equally spaced by a distance W that is much greater than the diameter D_o of the pipe. Therefore, the heat balance equations differ between those for water pipes and those between water pipes as shown in the geometrical configuration of the principal node of Fig. 4. The heat balance of the principal node at the water pipe is:

$$\dot{m}_{water} Cp_{water} \left(T_{principal}(y) - T_{principal}(y - W) \right) = \frac{k_{inner} L\ dy \left(T_{inner}(y) - T_{principal}(y) \right)}{\Delta x_{inner}}$$

$$if\ \frac{W}{2} + (p-1)W - \frac{d_0}{2} \le y \le \frac{W}{2} + (p-1)W + \frac{d_0}{2} \tag{7}$$

where p is an integer $1 \le p \le n$ standing for the water pipe number.

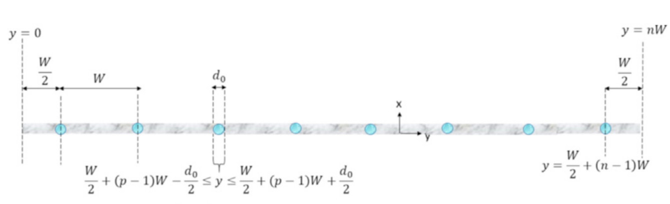

Fig. 4. Schematic of the principal node zone along y-axis.

The heat balance of the principal node between the water pipes is:

$$-k_{inner}\ dy\ L \frac{\left(T_{inner}(y) - T_{principal}(y) \right)}{\Delta x_{inner}} - k_{inner}\ \Delta x_{principal}\ Ldy \frac{\partial^2 T_{Principal}(y)}{\partial y^2}$$

$$if\ y \le \frac{W}{2} + (p-1)W - \frac{d_0}{2} \text{ or } y \ge \frac{W}{2} + (p-1)W + \frac{d_0}{2} \tag{8}$$

3.2.2.3. Outer node. The outer node represents the insulation medium considered adiabatic. Therefore, no heat flux occurs at the outer node leading to the following equation:

$$\frac{k_{outer} \left(T_{outer}(y) - T_{principal}(y) \right)}{\Delta x_{outer}} = 0 \tag{9}$$

3.2.2.4. Boundary conditions and mathematical model inputs. Although the mathematical model is simplified, and easy to solve using any numerical software; however, input parameters are needed. The input parameters are divided between (i) geometrical inputs like the size of PCRC, (ii) the thermal parameters like the supply water temperature T_{in} that should be given as the boundary condition at $y = 0$ of the principal node, and the room temperature T_r, (iii) the fluid parameters like the supply water flow rate $\dot{m}_{water}$ and the velocity of air over the radiant panel V_r that should be used to find Re number.

3.2.2.5. Numerical simulation of the mathematical model developed. The heat balance equations of PCRC with associated boundary conditions (Eqs. (1)–(9) are discretized along y using a finite volume methodology, where y-length of each three-node is divided into n_y nodes equally spaced by Δy. Central differencing is used for second order terms in energy equations. After introducing all the inputs and boundary conditions, assumptions will be made for the whole three-node model along y-axis, then the discretized equations will be solved using MATLAB software. The new values of temperatures are used in the next MATLAB simulation until that all energy equations are conserved in each grid and the maximum relative error between the new and old temperatures is not exceeding 10^{-5}. The grid size dy must ensure converged grid independent solution when using central differencing for the second order terms accounting for the conduction heat transfer. Thus, the numerical solution is repeated for different grid sizes to ensure that a grid-independent solution is obtained. The grid sizes chosen are $dy = 1$, $dy = 3$, and $dy = 5$ mm and the node temperatures along y are calculated. Since no significant difference is recorded between the finest and the largest grid size taken (less than 0.15%), $dy = 5$ mm is chosen for all the performed simulations. Once finished, the average temperature of the cooling radiant cubicle is computed as follows:

$$T_{crc} = \frac{\sum_1^{n_y} T_{inner}\left(i \right))}{n_y} \tag{10}$$

Table 3 summarizes all the geometrical inputs used for the cooling radiant cubicle.

Table 3
Geometrical dimensions of the cooling radiant cubicle used in the simulation.

Outer/inner tube diameter	20/16 mm [58]
Tube spacing	150 mm [58]
Water mass flow rate	1 kg/min
Inlet water temperature	12 °C
Thickness of aluminum sheet	5 mm [31]
Thickness of insulation	35 mm [59]

3.3. Integration between CFD and mathematical model

As mentioned in Section 3.1, the CFD model requires the knowledge of the PCRC surface temperature; thus, a simplified mathematical model is developed to compute the average temperature of PCRC where chilled water is flowing. However, as shown in Eqs. (1)–(9), in order to solve the equations of the mathematical model, T_r and V_r must be both known. T_r stands for the room air temperature and V_r is the velocity of air over the radiant panel. T_r is essential in solving the energy equation of each node, while V_r is required to compute Reynolds number *Re* that, in its turn, is used to find the convection coefficient as shown in equation 3 (a-b). Consequently, T_r and V_r must be considered as inputs for the developed mathematical model used to compute the average radiant cubicle temperature considered as a boundary condition in ANSYS, on one hand. On the other hand, T_r and V_r are also the outputs of CFD model as a result of simulating the space office equipped with radiant cooling cubicle. Therefore, both models are manually co-related together, and iterations between them must be used to come up with the converged solution. Fig. 5 summarizes the flow chart of the integration methodology between the CFD and the mathematical models. First, the average temperature of the radiant panel is assumed, then the CFD simulation is performed. Once done, the room temperature T_r and the velocity of air in the vicinity of the radiant panel V_r are found and entered to the mathematical model. Then, the new average temperature of the radiant panel is computed using Eq. (10) and compared to the value used at previous iteration. If the error is relatively small (<10^{-5}), then convergence occurs; if not, the iterations continue until convergence condition is attained. Then, the outputs of the integrated model such as the temperature at the vicinity of the occupant, the air velocity along with the metabolic rate, the rate of mechanical work, the mean radiant temperature, the relative humidity and the clothing insulation are all used as inputs for the thermal comfort models. In this study, the predicted mean vote (PMV) and the Percentage of People Dissatisfied (PPD) are calculated for two cases: the proposed case with PCRC and the conventional case without PCRC.

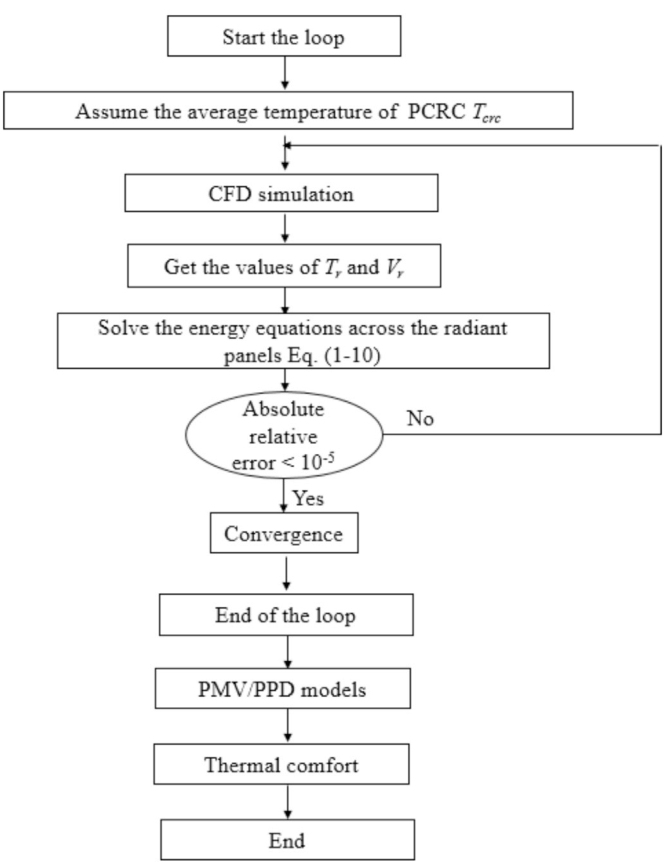

Fig. 5. Flow chart of research methodology.

3.4. Validation of the integrated model with published experiment

This section is devoted to test the validity of the integrated model by using experimental published data [31]. In this way, the ability of integrated model in capturing the thermal profile as well as the effect of PCRC in improving the thermal comfort zone at the vicinity of the office occupant is verified. Therefore, the integrated model inputs and conditions are adjusted to adhere for the published experimental conditions [31]. Then, the thermal profile near the occupant computed by the integrated model is compared to the published experimental data.

4. Results and discussion

In this section, the results of the integration between the CFD model and the mathematical model are presented. Comparison is made between the conventional case where no PCRC is implemented and the proposed study. Thermal comfort is tested by means of PMV and PPD. Afterwards, the proposed integration model is validated by comparing the findings to a published experiment [31]. Finally, the cumulative outflow is calculated and the pay-back period is computed.

4.1. Comparison between the conventional case and proposed case

In the conventional case, the same typical office geometrical dimensions presented in Table 1 are used. No PCRC is presented, and the air supply temperature is 14 °C. Since the objective of this study is to investigate the capability of PCRC in maintaining the occupant thermal comfort while increasing the air supply temperature and consequently decreasing the cooling load; thus, in the proposed case, the air supply temperature is increased to 18 °C. In the first simulation, an initial guess of PCRC exposed surface is assumed to be 14 °C. Then, iterations are achieved between CFD model and the mathematical model to achieve convergence. Only 300 iterations are needed for CFD convergence for each coupling during a maximum of 30 min, with a neglected computational time for the mathematical model solved on MATLAB. 4–5 couplings are needed between the CFD and the mathematical models to come up with the integrated model results.

Fig. 6 presents the results of both simulations: Fig. 6(a) illustrates the findings of the conventional case simulation when PCRC is not installed and the inlet temperature is 14 °C and Fig. 6(b) illustrates the findings of the proposed study where PCRC is placed at the vicinity of the occupant and the inlet temperature is 18 °C. It is shown in Fig. 6 that both systems present comfortable thermal zone at the vicinity of the occupant where the temperature does

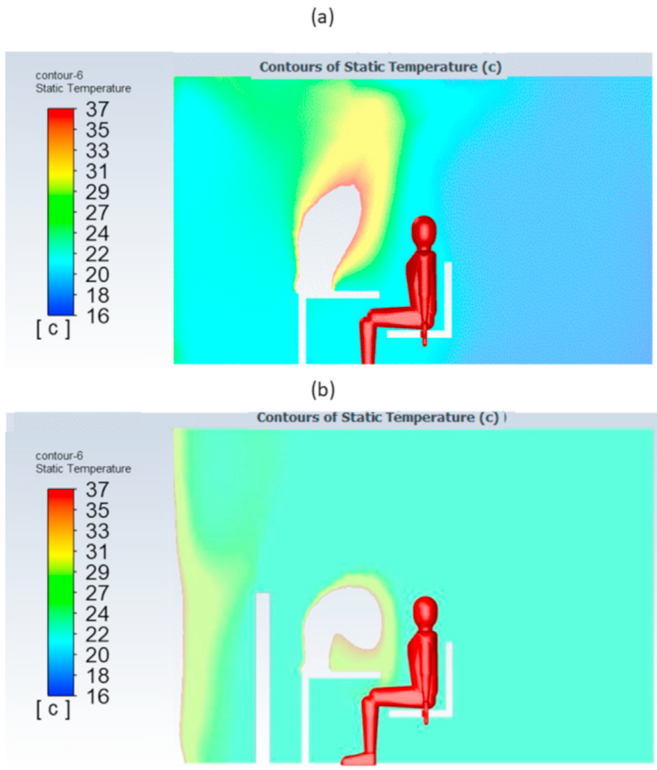

Fig. 6. Comparison between (a) the conventional case where no PCRC is presented and the supply air temperature is 14 °C and (b) the proposed study where PCRC is installed around the occupant and the supply air temperature is 18 °C.

not exceed 23 °C. The main difference recognized between both systems is that in the conventional system the temperature inside the typical office space (not at the occupant vicinity) is lower than the proposed system (22 °C compared to 24 °C). The main reason behind this finding is that in the conventional case the supply air temperature is relatively low (14 °C compared to 18 °C). However, this difference should not underestimate the effectiveness of the proposed system. Contrarily, it is shown that the presence of PCRC concentrates the cooling in the desired zone which is the vicinity of the occupant. Moreover, it is shown that the presence of PCRC reduces the thermal asymmetry around the occupant by reducing the thermal effect resulting from the presence of the computer.

Fig. 7 underlines the distribution of the cooling radiant cubicle in y-direction at the inner node exposed to the occupant zone. As shown in the figure, the temperature of the inner surface increases from $T = 12.1$ °C to $T = 16.21$ °C, resulting in an average of $T_{crc} = 14.3°C$.

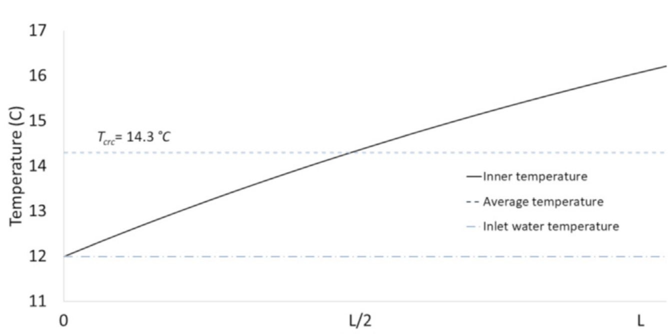

Fig. 7. Distribution of the inner temperature along y-axis attaining an average temperature of 14.3 °C.

Fig. 8 represents the temperatures of the principal nodes at the water pipes level. As shown in the figure, the chilled water enters the system at a low temperature of 12 °C. Then, the water temperature increases while exchanging heat with the inner nodes from 12 °C to around 16 °C. The energy absorbed by the chilled water flowing is equal to the energy absorbed from the space by radiation and convection to maintain the thermal comfort of the occupant. Different factors play important roles in increasing or decreasing this absorbed energy. For instance, the water flow rate, the inlet temperature of water, the dimensions of the cooling radiant cubicle, and the velocity at the vicinity of radiant panels can all affect the energy absorbed from the radiant cubicle.

In order to investigate the thermal performance of the proposed study and its ability in delivering human thermal comfort, the predicted mean vote (PMV) and the predicted Percentage of People Dissatisfied (PPD) of both cases are calculated using an online calculator [59]. The inputs to the online calculator involve the metabolic energy production (58–232 W/m^2), the rate of mechanical work (normally 0), the ambient air temperature (10–30 °C), the mean radiant temperature (often close to ambient air temperature), the relative air velocity (0.1–1 m/s), the air relative humidity, and the basic clothing insulation (where 1 clo = 0.155 W/m^{2}K).

For both the conventional and the proposed cases, the metabolic rate is considered 58 W/m^2, the rate of mechanical work is zero, the indoor relative humidity is considered 50%, and the sedentary thermal manikin occupant is wearing medium clothing (1 clo).

Regarding the air velocity and temperature around the occupant, they are obtained by doing the average from CFD simulation taken as 1 cm far from the thermal manikin. Table 4 presents the values of PMV and PPD for both cases. Results show that the proposed system presents also thermally comfortable zone since $-0.5 \leq PMV \leq 0.5$ and $PPD \leq 20\%$. It is also shown that the conventional case is closer to cool conditions while the proposed case is closer to warm conditions. However, PPD of the proposed study (5.6%) is even better than the conventional case (8.1%). From here comes the importance of such system in minimizing the cooling energy by increasing the supply air temperature and maintaining a personalized thermal comfort at the occupant vicinity by means of radiant cooling.

4.2. Model validation with published experiment

To ensure the validity of the proposed model developed, it is indispensable to find a published experiment that combine the radiant cooling panel cubicle with a conventional HVAC system. It is found that Vaibhav Rai khare and his team were the pioneer in suggesting such system and in studying the personalized cooling system using the principle of radiant cooling integrated with the conventional all-air system to achieve better thermal environment at the workspace [31, 32]. They even combine in further studies,

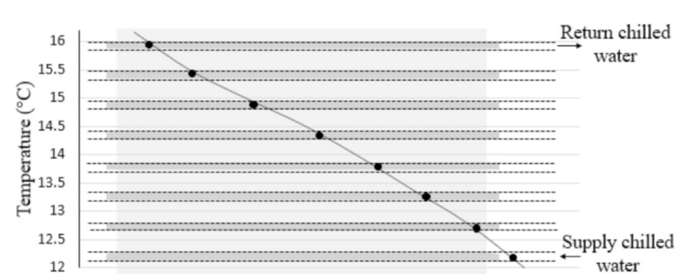

Fig. 8. Distribution of the principal temperature along the water pipes.

Table 4
PMV and PPD for conventional and proposed cases.

	Thermal comfort parameters			
	Air temperature around the occupant	Air velocity around the occupant	PMV	PPD
Conventional case	22	0.1	−0.39	8.1
Proposed case	24	0.06	0.16	5.6

the radiant cooling system with other radiant systems like the radiant ceiling conditioning system and found that this combination could also fulfill the requirement of thermal comfort in an efficient way [19, 33]. Nevertheless, since in this study, the performance of PCRC combined with conventional HVAC is tested, then the appropriate experiment is selected [31]. In this experiment, Fig. 9 displays the schematic of their experimental setup.

In this experiment, the chilled water flows through copper tubes and the heat transfer from the working fluid is absorbed by radiation and conduction. The tubes are mounted on the aluminum sheet in a serpentine configuration. The thin Aluminum sheet (<0.5 mm) is used to wrap the copper tubes and prolonged at the ends to offer efficient heat transfer. The room in which radiant cubicle is a single room of 13 m^2 surface area with concrete exterior walls and floor and having a conventional air-conditioning system (split located at the wall) with an inlet air velocity of 3 m/s and supply air temperature kept constant for 18 °C while the inlet water temperature is 14 °C. For the internal walls and floor, the heat transfer is around 17 W/m^2, and the occupant is simulated as heat flux of 55 W/m^2. Therefore, these experimental conditions are used to adjust the integrated model inputs for the sake of validation.

However, the only difference between the experimental and the integrated model conditions is that the experiment is conducted under transient conditions (hourly). Therefore, in order to test the validity of the model in capturing the thermal profile at the vicinity of the occupant, the average temperature over the time is computed and compared to the numerical simulation results. The result of the experiment shows that the air at the vicinity of the occupant lies between 23.8 °C and 24.22 °C with a time average of 24.13 °C. Fig. 10 illustrates the results of the simulation after running the model under the published experimental conditions and geometry. It is shown that in this case, the air temperature at the vicinity of the occupant is between 23 °C and 24 °C which is close to the experimental finding with a maximum relative error of 5%.

Fig. 9. Schematic of the published experiment performed by Khare et al. [31].

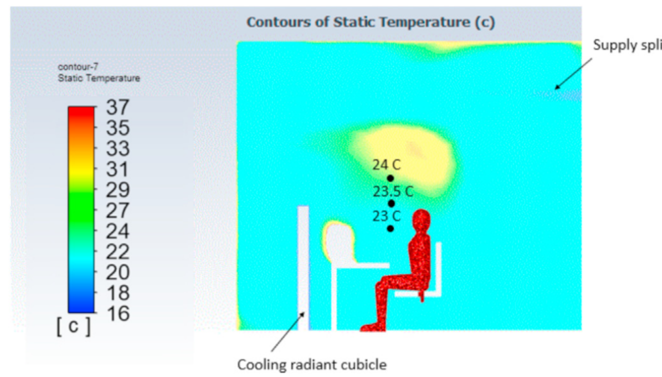

Fig. 10. ANSYS simulation based on the published experimental set up.

4.3. *Economic implications and benefits of the proposed system*

In this section, an economic feasibility study of the proposed PCRC system is established to evaluate its pay-back period and energy savings over the conventional cooling system case. For this reason, the cumulative outflow and the net present value (NPV) of both systems (conventional and proposed) are assessed. The real discount rate of return is selected as 2% and the period is considered as 20 years. Since both systems have the same mechanical cooling system used in the office, its initial cost is not included. However, since the PCRC is presented only in the proposed study, its initial cost is considered as the initial cost of the proposed case and it is equal to 390$ as shown in Table 5.

To determine the yearly electrical consumption, the cooling load is estimated over the whole year for both cases. The results show a total cooling load of 5.7 MWh/year in the conventional case compared to 2.83 MWh/year for the proposed PCRC case (50% less) when the supply temperature is increased from 14 °C to 18 °C. Furthermore, all the electrical system components consume around 1.7 MWh/year in the conventional case. However, since the proposed system has additional electrical consumption for the portable chiller and the pump; therefore, the proposed system components consume 876 KWh/year more electricity.

The average tariff rate of electricity in Doha is currently around 3 US cent/kWh [65] with a 2% assumed electricity price growth rate. Therefore, the cumulative outflow of the conventional system over 20 years is 4350$, compared to 3570 $ for the proposed system inducing a resultant reduction of 18%.

Finally, the payback period of the proposed system was

Table 5
Geometrical dimensions of the cooling radiant cubicle used in the simulation.

Copper tubes	100 $ [60]
Aluminium sheet	102 $ (17 $/m^2) [61]
Insulation	48 $ (8$/m^2) [62]
Water pump	10 $ [63]
Portable water chiller	130 $ [64]

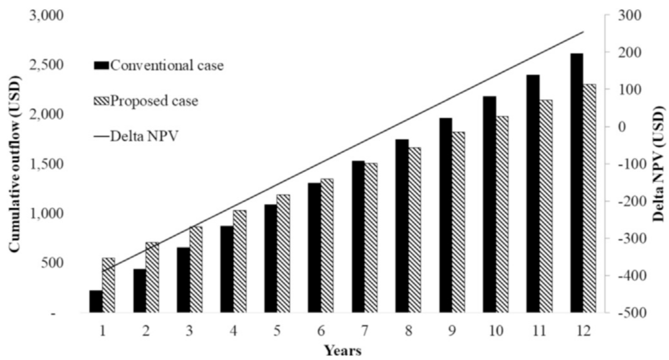

Fig. 11. Cumulative outflow and delta NPV ($) for the proposed system compared to the conventional system.

computed by plotting delta net present value (NPV) as shown in Fig. 11. It is shown that the pay-back period occurs between 6 and 7 years when delta NPV becomes positive.

5. Future work

The future work will be based on conducting an experiment that simulates the PCRC system in an environmental chamber and performing an uncertainty analysis as well as a parametric study. This will be followed by an optimization study using artificial intelligence network and multi-objective genetic algorithm to address the optimal design parameters that can minimize the energy consumption while maximizing the thermal comfort.

6. Conclusion

A new personalized cooling radiant cubicle PCRC is established and investigated to decrease the cooling load of office spaces especially in hot climates such as Doha, Qatar. The PCRC system is based on radiant panels where water flows at relatively low temperature. A CFD model integrated with a simplified mathematical model is used to simulate the PCRC thermal performance. The proposed system is assessed based on the simulations of the integrated model compared to the conventional case where PCRC is not installed. The results show that when PCRC is installed, HVAC system is allowed to work at higher thermostat temperature without compromising the occupant thermal comfort, resulting in a reduction of the associated space-cooling load. The key findings of the study are summarized as follows:

1. In hot climates, it is shown that the presence of PCRC concentrates the cooling in the desired zone which is the vicinity of the occupant and helps attaining the occupant thermal comfort.
2. The developed model succeeds in simulating the thermal effect of installing PCRC in the office with a maximum relative error of 5% compared to published experiment.
3. The results show a total cooling load of 5.7 MWh/year in the conventional case compared to 2.83 MWh/year for the proposed PCRC case (50% less) when the supply temperature is increased from 14 °C to 18 °C.
4. The cumulative outflow of the conventional system over 20 years is 4350$, compared to 3570 $ for the proposed PCRC system inducing a resultant reduction of 18%. and a payback period between 6 and 7 years.

Declaration of competing interest

The authors declare that they have no known competing financial interests or personal relationships that could have appeared to influence the work reported in this paper.

Acknowledgement

The authors would like to acknowledge the financial support of Qatar University.

References

[1] Kim J, Song D, Kim S, Park S, Choi Y, Lim H. Energy-saving potential of extending temperature set-points in a VRF air-conditioned building. Energies 2020;13(9):2160.

[2] Freire RZ, Oliveira GH, Mendes N. Predictive controllers for thermal comfort optimization and energy savings. Energy Build 2008;40(7):1353–65.

[3] Ghahramani A, Zhang K, Dutta K, Yang Z, Becerik-Gerber B. Energy savings from temperature setpoints and deadband: quantifying the influence of building and system properties on savings. Appl Energy 2016;165:930–42.

[4] Hoyt T, Arens E, Zhang H. Extending air temperature setpoints: simulated energy savings and design considerations for new and retrofit buildings. Build Environ 2015;88:89–96.

[5] Aryal A, Becerik-Gerber B. Energy consequences of Comfort-driven temperature setpoints in office buildings. Energy Build 2018;177:33–46.

[6] Van Hoof J. Forty years of Fanger's model of thermal comfort: comfort for all. Indoor Air 2008;18(3):182–201.

[7] Kim J, Schiavon S, Brager G. Personal comfort models–A new paradigm in thermal comfort for occupant-centric environmental control. Build Environ 2018;132:114–24.

[8] Van Marken Lichtenbelt W, Hanssen M, Pallubinsky H, Kingma B, Schellen L. Healthy excursions outside the thermal comfort zone. Build Res Inf 2017;45(7):819–27.

[9] Verhaart J, Veselý M, Zeiler W. Personal heating: effectiveness and energy use. Build Res Inf 2015;43(3):346–54.

[10] Brager G, Zhang H, Arens E. Evolving opportunities for providing thermal comfort. Build Res Inf 2015;43(3):274–87.

[11] Luo M, Arens E, Zhang H, Ghahramani A, Wang Z. Thermal comfort evaluated for combinations of energy-efficient personal heating and cooling devices. Build Environ 2018;143:206–16.

[12] Xie J, Li H, Li C, Zhang J, Luo M. Review on occupant-centric thermal comfort sensing, predicting, and controlling. Energy Build 2020:110392.

[13] Zhang H, Bauman F, Arens E, Zhai Y, Dickerhoff D, Zhou X, Luo M. Reducing building over-cooling by adjusting HVAC supply airflow setpoints and providing personal comfort systems. 2018.

[14] Melikov AK, Skwarczynski MA, Kaczmarczyk J, Zabecky J. Use of personalized ventilation for improving health, comfort, and performance at high room temperature and humidity. Indoor Air 2013;23(3):250–63.

[15] Watanabe S, Shimomura T, Miyazaki H. Thermal evaluation of a chair with fans as an individually controlled system. Build Environ 2009;44(7):1392–8.

[16] Hatoum O, Ghaddar N, Ghali K, Ismail N. Experimental and numerical study of back-cooling car-seat system using embedded heat pipes to improve passenger's comfort. Energy Convers Manag 2017;144:123–31.

[17] Pasut W, Zhang H, Arens E, Zhai Y. Energy-efficient comfort with a heated/cooled chair: results from human subject tests. Build Environ 2015;84:10–21.

[18] Zhang H, Arens E, Taub M, Dickerhoff D, Bauman F, Fountain M, Pasut W, Fannon D, Zhai Y, Pigman M. Using footwarmers in offices for thermal comfort and energy savings. Energy Build 2015;104:233–43.

[19] Khare VR, Garg R, Mathur J, Garg V. Thermal comfort analysis of personalized conditioning system and performance assessment with different radiant cooling systems. Energy and Built Environment; 2021.

[20] Srivastava P, Khan Y, Mathur J, Bhandari MS. Analysis of radiant cooling system integrated with cooling tower for composite climatic conditions. Oak Ridge, TN (United States): Oak Ridge National Lab.(ORNL); 2018.

[21] Zhang F, Guo HA, Liu Z, Zhang G. A critical review of the research about radiant cooling systems in China. Energy Build 2021;235:110756.

[22] Laouadi A. Development of a radiant heating and cooling model for building energy simulation software. Build Environ 2004;39(4):421–31.

[23] Zhou G, Jing H. Thermal performance of a radiant floor heating system with different heat storage materials and heating pipes. Appl Energy 2015;138:648–60.

[24] Karacavus B, Aydin K. Numerical investigation of general and local thermal comfort of an office equipped with radiant panels. Indoor Built Environ 2019;28(6):806–24.

[25] Xie D, Wang Y, Wang H, Mo S, Liao M. Numerical analysis of temperature non-uniformity and cooling capacity for capillary ceiling radiant cooling panel. Renew Energy 2016;87:1154–61.

[26] Xie D, Wang C, Yu CW, Wang Y, Wang H. Performance of capillary ceiling cooling panel on ceiling surface temperature and indoor thermal environment. Indoor Built Environ 2020;29(6):881–94.

[27] Mustakallio P, Kosonen R, Korinkova A. Full-scale test and CFD-simulation of radiant panel integrated with exposed chilled beam in heating mode. In: Building simulation. Tsinghua University Press; 2017. p. 75–85.

[28] Catalina T, Virgone J, et Kuznik F. Evaluation of thermal comfort using

combined CFD and experimentation study in a test room equipped with a cooling ceiling. Build Environ 2009;44(8):1740–50.
[29] Du J, Chan M, Deng S. An experimental study on the performances of a radiation-based task/ambient air conditioning system applied to sleeping environments. Energy Build 2017;139:291–301.
[30] Du J, Chan M, Pan D. A numerical study on the effects of design/operating parameters of the radiant panel in a radiation-based task air conditioning system on indoor thermal comfort and energy saving for a sleeping environment. Energy Build 2017;151:250–62.
[31] Khare V, Sharma A, Mathur J, Bhandari MS. Development of personalized radiant cooling system for an office room. Oak Ridge, TN (United States): Oak Ridge National Lab.(ORNL); 2015.
[32] Khan Y, Khare VR, Mathur J, Bhandari M. Performance evaluation of radiant cooling system integrated with air system under different operational strategies. Energy Build 2015;97:118–28.
[33] Garg R, Khare VR, Mathur J, Garg V. Performance evaluation of personalized radiant conditioning system for cooling mode. Build Simul 2017:2728–34. 2017.
[34] Yuan Y, Zhang X, Zhou X. Simplified correlations for heat transfer coefficient and heat flux density of radiant ceiling panels. Sci Technol Built Environ 2017;23(2):251–63.
[35] Andrés-Chicote M, Tejero-González A, Velasco-Gómez E, Rey-Martínez FJ. Experimental study on the cooling capacity of a radiant cooled ceiling system. Energy Build 2012;54:207–14.
[36] Fatchurrohman N, Chia ST. Performance of hybrid nano-micro reinforced mg metal matrix composites brake caliper: simulation approach. In: IOP conference series: materials science and engineering, vol. 257; 2017, 012060. 1.
[37] Makhoul A, Ghali K, Ghaddar N. Investigation of particle transport in offices equipped with ceiling-mounted personalized ventilators. Build Environ 2013;63:97–107.
[38] Zhang Z, Chen Q. Experimental measurements and numerical simulations of particle transport and distribution in ventilated rooms. Atmos Environ 2006;40(18):3396–408.
[39] Makhoul A, Ghali K, Ghaddar N. Low-mixing coaxial nozzle for effective personalized ventilation. Indoor Built Environ 2013;22(3):508–19.
[40] Makhoul A, Ghali K, Ghaddar N. Desk fans for the control of the convection flow around occupants using ceiling mounted personalized ventilation. Build Environ 2013;59:336–48.
[41] ANSYS software: ANSYS Inc. http://www.ansys.com/.
[42] Zheng X, Han Y, Zhang H, Zheng W, Kong D. Numerical study on impact of non-heating surface temperature on the heat output of radiant floor heating system. Energy Build 2017;155:198–206.
[43] Ning B, Chen Y, Liu H, Zhang S. Cooling capacity improvement for a radiant ceiling panel with uniform surface temperature distribution. Build Environ 2016;102:64–72.
[44] Zhang C, Heiselberg PK, Chen Q, Pomianowski M. Numerical analysis of diffuse ceiling ventilation and its integration with a radiant ceiling system. Build Simul 2017;10(2):203–18.
[45] Karacavus B, Aydin K. Numerical investigation of general and local thermal comfort of an office equipped with radiant panels. Indoor Built Environ 2019;28(6):806–24.
[46] Peng P, Gong G, Deng X, Liang C, Li W. Field study and numerical investigation on heating performance of air carrying energy radiant air-conditioning system in an office. Energy Build 2020;209:109712.
[47] Du J, Chan M, Pan D, Deng S. A numerical study on the effects of design/operating parameters of the radiant panel in a radiation-based task air conditioning system on indoor thermal comfort and energy saving for a sleeping environment. Energy Build 2017;151:250–62.
[48] Lin Z, Deng S. A study on the thermal comfort in sleeping environments in the subtropics—measuring the total insulation values for the bedding systems commonly used in the subtropics. Build Environ 2008;43(5):905–16.
[49] Selmi M, Tag IA. Economic and thermal performance of thermostone in Qatar. 1996.
[50] http://shared4.info/architecture/qcs/index.php?option=com_content&view=category&id=32.
[51] Kharseh M, Hassani F, Al Khawajah M. The possibility to lower building energy consumptions in Qatar. October. In: Qatar foundation annual research forum volume 2012. Hamad bin Khalifa University Press (HBKU Press; 2012, EEP38. Issue 1 (Vol. 2012, No. 1.
[52] https://15shp.com/15SHP_Downloads_Specs.pdf.
[53] https://smallbusiness.chron.com/laptop-vs-pc-power-consumption-79347.html.
[54] Haddad S, Osmond PAUL, King STEVE. Metabolic rate estimation in the calculation of the pmv for children. In: 47th international conference of the architectural science association. The Architectural Science Association Australia; 2013. p. 241–50. November.
[55] Incropera FP, Dewitt DP. Fundamentals of heat and mass transfer. J. Wiley; 2002.
[56] Rohsenow Warren M, Hartnett James P, Cho Young I. Handbook of heat transfer. McGraw-Hill; 1998.
[57] Drojetzki L, Wojtkowiak J. Ceiling mounted radiant panels–calculations of heat output in heating and cooling application. In: E3S Web of conferences, vol. 44; 2018, 00035.
[58] Oubenmoh S, Allouhi A, Mssad AA, Saadani R, Kousksou T, Rahmoune M, Bentaleb M. Some particular design considerations for optimum utilization of under floor heating systems. Case Stud Therm Eng 2018;12:423–32.
[59] Habchi C, Ghali K, Ghaddar N, Shihadeh A. Chair fan-enhanced displacement ventilation for high IAQ: effects on particle inhalation and stratification height. Build Environ 2015;84:68–79.
[60] https://www.alibaba.com/product-detail/2016-High-quality-20mm-copper-pipe_1600168149945.html?spm=a2700.pc_countrysearch.main07.168.773132d5z8hsS7.
[61] https://www.haomeicn.com/a/what-is-the-price-of-a-3mm-thick-aluminium-sheet.html.
[62] https://enviroshop.com.au/pages/home-insulation.
[63] https://www.alibaba.com/product-detail/Good-Selling-Peristaltic-Air-Pump-1_62466048544.html?spm=a2700.7724857.normal_offer.d_image.4ddb5b11neHqzL.
[64] https://www.alibaba.com/product-detail/water-chiller-cw3000-for-CO2-Laser_60740250237.html?spm=a2700.galleryofferlist.normal_offer.d_image.1180515eZTJE9A&s=p.
[65] Mohandes N, Sanfilippo A, Al Fakhri M. Modeling residential adoption of solar energy in the Arabian Gulf Region. Renew Energy 2019;131:381–9.